Macromolecules **2002,** *35,* 271−277

Stress Relaxation in Transient Networks of Symmetric Triblock Styrene−Isoprene−Styrene Copolymer

A. Hotta, S. M. Clarke,[†] and E. M. Terentjev*

Cavendish Laboratory, University of Cambridge, Madingley Road, Cambridge CB3 0HE, U.K.

Received November 17, 2000; Revised Manuscript Received September 4, 2001

ABSTRACT: We study thermoplastic elastomers of triblock copolymers, of the form polystyrene−polyisoprene−polystyrene (SIS), where the microphase-separated PS blocks act as physical cross-links for the PI elastic network. Two compositions are examined: one with micellar cubic and the other with hexagonal cylindrical morphology of PS. Remarkably, the long-time stress relaxation is very similar; it reveals a continuous crossover between the typical response of a classical rubber at low temperatures and that of an entangled melt at high temperatures, above the T_g of polystyrene micelles. However, at a temperature T^* well below the glass transition T_g(PS), the stress relaxation experiences a crossover between the classical rubber power law and a much faster relaxation above T^*, which follows a stretched-exponential law for the extension modulus $E(t) \sim b \exp[-(t/\tau)^{0.2}]$. Time−temperature superposition is possible at all temperatures below T_g(PS), but the classical WLF equation could not be made to describe the shift factors. These results are interpreted in terms of transient (breakable under stress) cross-links and a local stress relief when PS chains are pulled out of the glassy micelles, with the characteristic time of PS release at each temperature below T_g(PS) determining the mechanical response at a given strain rate.

Introduction

The stress relaxation of cross-linked rubbers is a problem that is still not well understood and is currently attracting significant experimental and theoretical interest. The time dependence of the effective extension modulus $E(t)$, defined by the stress−strain convolution $\sigma(t) = \int E(t - t')(\mathrm{d}/\mathrm{d}t')\epsilon(t')\,\mathrm{d}t'$, contains much information about the internal physics of random polymer networks and can provide a sensitive test for a variety of theoretical models of polymer rheology. Despite 50 years of investigations into rubber behavior, there are still very few experimental results on long time relaxation. The classic work in this field is that of Chasset and Thirion[1] and Ferry et al.,[2] where a power-law relaxation $E(t) \sim E_0[1 - (t/t_0)^{-m}]$ has been established experimentally. The theoretical model of Curro et al.[3,4] suggested that such behavior could be due to the relaxation of loops and free dangling ends of polymer networks.

Transient networks, that is, polymer gels where the cross-links could be broken (and sometimes reconnected), spontaneously or under stress, are also attracting much current interest. The reasons range from applied aspects of food colloids[5] to the fundamental microstructure and viscoelastic properties of *thermoreversible gels*,[6] in particular, *telechelic* networks formed by triblock copolymers with short immiscible end blocks (the effective cross-links).[7] The interest in elastic properties of transient networks with breakable cross-links dates back to the early work of Thomas[8] and Flory,[9] which, at that time, mostly concentrated on hydrogen-bonding cross-links. In the present work we have studied a thermoreversible elastomer system where the effective strength of cross-linking is temperature-dependent, varying between a rigid limit of “permanent cross-links” to a weak limit when network strands are held together by only a weak potential. In this manner we could sweep the behavior from an essentially permanently cross-linked classical rubber material to the one where the cross-links are at best transient. This is achieved with symmetric triblock copolymers of the form polystyrene−polyisoprene−polystyrene (PS−PI−PS, or SIS) melt, where the minority PS blocks phase-separate and act as physical cross-links for the PI elastic network forming the continuous majority phase. Depending on the copolymer composition, the morphology of such phase separation may vary. A large industry of research has examined this question over the years (see refs 10−12). The morphology and the phase boundaries of an SIS system are well-known; we are particularly interested in the cubic phase of spherical PS micelles, at the lower concentration (14% in our case), and the hexagonally packed cylindrical PS regions at a higher (17%) proportion of PS in the copolymer composition (see Figure 1).

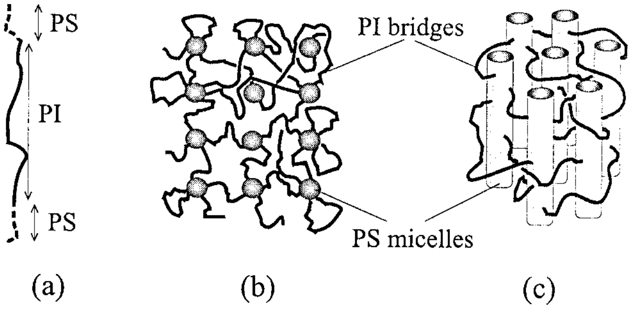

Figure 1. Sketch of SIS triblock copolymer (a) and the morphology of its phase separation: the cubic phase of spherical micelles in the 14% PS material (b) and the hexagonally packed phase of cylindrical micelles in the 17% PS material (c). Long PI bridges interconnect the PS micelles, making an elastomer network with effective multifunctional cross-links.

In this article we are concerned with the mechanical stress relaxation in an effective elastomer formed by the

---

[†] Present address: The BP Institute, University of Cambridge, CB3 0EZ, U.K.

* Corresponding author. E-mail emt1000@cam.ac.uk.

10.1021/ma001976z CCC: $22.00

microphase-separated SIS copolymer melt. In simple terms, it is expected that below the glass transition of PS micelles one should find a mechanical behavior characteristic of a permanent rubbery network of PI, while above this point, T_g(PS), the PS micelles would not be expected to support the forces of the deformed PI network, and the material would become a thermoplastic gel. Of course, there are two more characteristic temperatures in such a system: below the glass transition of the PI matrix, T_g(PI), the material would become an ordinary polymer glass, while above the phase separation binodal a homogeneously mixed PS−PI melt would result. Here we are not interested in these limiting regimes and concentrate on the region around and below T_g(PS), investigating the role of cross-links on the rubbery PI network.

We will demonstrate that there is one more characteristic temperature in the system, $T^* \sim 30$ °C, well below $T_g(\mathrm{PS}) \sim 70$ °C. Below T^* one finds the expected rheological response of a permanently cross-linked rubber, while above T^* the supposedly glassy PS micelles act as breakable linkages—by a mechanism we propose to be PS chain pullout under force from their micellar aggregates. As a result, in this regime we find a faster relaxation of stress, described by a stretched-exponential law, and nonrecoverable change of sample shape (creep) after a long period of deformation, a “permanent set”. However, the total density of effective cross-links remains constant at each temperature, indicating that although the effective micellar cross-links are breaking under stress, the released chains are reconnecting to different network strands. We argue that there is a characteristic time scale of PS chain pullout from a glassy matrix, $\tau_{\mathrm{PS}}(T)$, which moves into the experimentally accessible window above T^*.

Our results and general observations are qualitatively close to the recent report of Sato et al.,[13] who also studied the mechanical relaxation in SIS system. Their system has been very different: the high 28% PS content, much shorter chains, and the 50% tetradecane solvent. All these factors must have dramatically affected the relaxation mechanisms. In addition, the authors of refs 13 and 14 only perform the dynamic measurements with the lowest frequency of ~ 0.01 s^{-1}, while we focus on the truly long time relaxation processes. Despite these differences, there are remarkable similarities in the experimental results: Sato et al. also report a crossover temperature $T^* \sim 30$ °C and a wide distribution of relaxation times (confirmed by our stretched exponential relaxation law, see below). The authors attribute their observations to the effect of a PS chain pullout from the segregated micelles. We also consider this a primary relaxation mechanism, except that we find evidence that the chain pullout occurs even below T_g(PS). The fact that there are so many qualitative similarities, despite great differences in the systems studied, gives comfort and hope that the results reported here are even more universal than one might expect.

2. Experimental Section

The step-strain relaxation measurements were made on a custom-built stretching device described previously.[15] The temperature compensated force transducer was obtained from Pioden Controls Ltd. For studies of very long time relaxation good temperature control is essential. In our device the temperature was carefully held to within ±0.3 °C of the target value over prolonged intervals of time by using two isothermal boxes with active temperature control. There was no attempt to control humidity. Both the force and the temperature data were logged and interpreted by a computer directly interfacing with the stretching device.

Table 1. Molecular Weights (Total and That of Each Terminal PS Block) of the Two Materials under Study and the Corresponding Glass Transition Temperatures[a]

sample	total M_w	$M_w(^1/_2\mathrm{PS})$	T_g(PI), °C	T_g(PS), °C
14% PS	245 000	17 150	−50	65
17% PS	160 000	13 600	−55	72

[a] The glass transition of PI in the disperse system such as microphase-separated SIS is broad and its value is taken, approximately, as the inflection point of the thermogram.

The SIS triblock copolymers used here was obtained from Aldrich Chemical Corp. with a PS/PI molecular weight ratio of 14% and 17%. We performed gel permeation chromatography (GPC) to verify the molecular weight M_w and polydispersity of materials, which was less than 1.1 (as one usually expects in a living anionic polymerization). The material data are listed in Table 1. One should recognize that the 14% PS sample has much longer overall length of the middle PI-block (210 700, in comparison with 132 800 for 17% PS material). This will account for a significantly lower elastic modulus of the resulting elastomer. In the following study we are not concerned with the absolute magnitude of elastic response, but rather in relative values describing relaxation dynamics.

Differential scanning calorimetry (DSC) measurements (Perkin-Elmer Pyris 1 DSC) were used to characterize the phase transformations in the materials. The two glass transition temperatures of the SIS samples were unambiguously determined (cf. Table 1) with no additional thermal transitions between. We also determined the T_g values for pure PI and PS samples of nearly the same molecular weight homopolymers as the components of the SIS block copolymer used here. These were approximately −63 and 92 °C respectively for PI and PS. This kind of difference is expected and is consistent with the composition of PS- and PI-majority regions in the phase-separated state: there is a small concentration of the minority component in each of these regions, which acts as an impurity and shifts the corresponding glass transition. To confirm that any other impurities present were not distorting the results, repeated reprecipitation from toluene and methanol was used to purify the copolymer. Similar results for all transition temperatures were obtained with this purified material as those of the as-received samples.

Another aspect of glass transition shifts is the size of phase-separated PS micelles. It is well-known that there would be a size effect in the measured T_g; see refs 16 and 17 for example. In our case, the small-angle synchrotron X-ray diffraction data confirm the size of micelles (in both spherical cubic and cylindrical hexagonal phases) to be around ∼6 nm, very narrowly dispersed. From the comparison of glass transition temperatures, it appears that this size was too big to give any additional significant shift in T_g’s.

Thin samples for the stress relaxation measurements were prepared by pressure molding. The particles of SIS, as received, were sandwiched between the two sheets of PTFE films covered by metal plates. Metal spacers were used to control the thickness of the samples. The molding temperature was 135 °C, well above the T_g of PS. Initially the samples were heated under a pressure of 300 [lbf/in.^{2}] for 60 min to a thickness of 1 mm and then allowed to cool slowly to the room temperature. Subsequently, the samples were remolded at the same temperature and pressure for 30 min to a thickness of ∼0.15 mm. After this procedure the samples were flat, homogeneous, and transparent with no sign of the original particulate form. The samples were cut with a razor blade into a rectangular shape of approximately 3 × 25 × 0.15 mm (narrow elongated strips minimize edge effects during extensional deformation). The thickness, length, and width of samples were measured by a micrometer at three points; the average of the three values was used to calculate the stress. Samples were clamped at two ends using thermally resistant polyimide tape.

The samples were extended in a step-strain fashion by 25%, measured with a micrometer. This choice of fixed deformation is rather arbitrary, directed by the need to measure higher forces to increase accuracy but avoiding too high strains where even a classical rubber would behave nonlinearly. The Appendix to this paper provides additional information on the stress−strain relationships and strain-dependent relaxation. The force on the sample and the temperature were measured as a function of time for 2 days after the deformation was imposed. These measurements were repeated for a number of temperatures between 4 and 90 °C. The stress values, obtained in arbitrary units, were calibrated with weights at different temperatures. Because the stress sensor used here was specially temperature compensated, there was only a small adjustment in the calibration with temperature. Data presented here correspond to an engineering strain of 1.25 ($\lambda = L/L_0$, where L_0 is the unstretched length and the L is the fixed extended length). Stress values will be presented as nominal stress (σ, equal to the measured force divided by the original cross section of the sample).

The natural, unstretched length of the samples, L_0, is an important parameter—both to calculate the correct strain value and, after the end of stretching experiment, to determine whether the sample recovers its shape elastically. Each time, this length was determined experimentally from a very small amplitude stress−strain measurement. The samples were then extended to a strain of $\lambda = 1.25$ in 45 s and kept at constant temperature for 2 days to monitor relaxation. The sample preparation history, including the rate of imposed strain and the total time of relaxation, was kept constant throughout the whole series of experiments.

3. Results

The two samples under investigation show very similar mechanical relaxation, despite their rather different "cross-linking morphology". We shall return to the discussion of possible reasons and the key factors determining such a response in the end of this article. This section begins with the raw data on stress relaxation, after a 25% step strain, at different temperatures between 4 and 90 °C (Figure 2). The axes in this figure are logarithmic time (corresponding to a maximum of 2 days) and logarithmic stress, such that a power-law response would appear as a straight line in the plot. Since the engineering strain was the same for all experiments, the measured stress $\sigma(t)$ is effectively the same as the effective modulus $E(t)$; however, we shall see later that in many cases the primary reason for relaxation is the underlying plastic deformation reducing the effective strain in the network. As expected, the stress values fall with increasing time and temperature. The stress relaxation curves below 30 °C are essentially straight lines and parallel with each another. At a temperature $T^* \sim 30$ °C, the relaxation curve deviates from this straight line (power law) behavior. Above T^* but below T_g(PS), the relaxation curves curve downward, indicating a faster than power-law decay.

Above T_g(PS) only a small relaxation is evident, with both samples essentially acting like a viscoelastic liquid at long times. Although this regime is not the subject of our work, we remark that the stress relaxation in such soft "telechelic" network (theoretically studied in, e.g., ref 7) closely follows the power law $\sigma(t) \sim at^{-1/2}$. (A dashed line next to the high-temperature data on both plots shows the power-law slope of −1/2.) Let us mention here that this type of response, also represented by a $E^*(\omega) \sim (i\omega)^{1/2}$ frequency variation, is seen in a number of microphase-separated copolymer melts (see ref 18). It seems that, although the quoted theory addresses the lamellar phase while we have spherical and cylindrical micelles, the −1/2 power-law is a more general and characteristic rheological feature of a complex fluid with an energy barrier for internal reorganization.

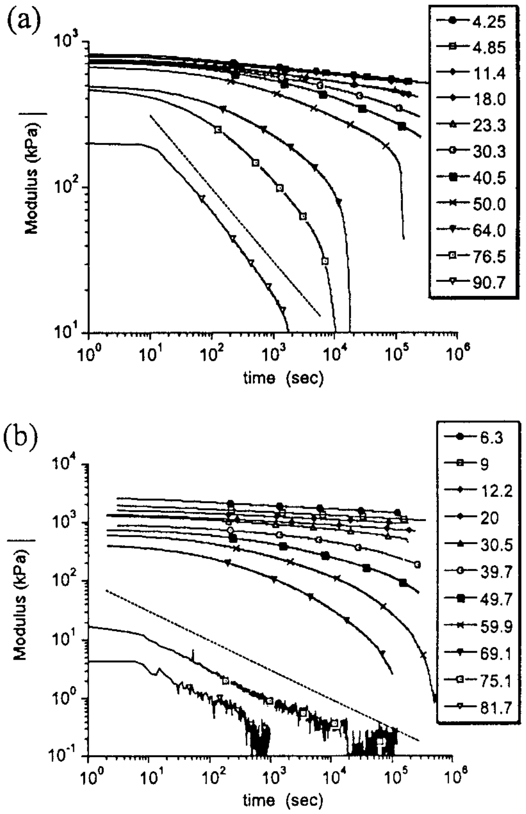

Figure 2. Results of the stress relaxation experiments at a sequence of increasing temperatures (shown as legends on plots) for the sample 14% PS (a) and 17% PS (b). Clearly, the high-temperature regime above the glass transition of PS micelles is viscoelastic: a dashed line showing the power-law exponent of $-{}^1/_2$ is drawn near the data for both materials. The amount of stress relaxation in the regime below T_g(PS) increases with increasing temperature and invites time−temperature superposition analysis.

3.1. Time−Temperature Superposition.

Figure 3 shows the master curves of the stress relaxation obtained by shifting each relaxation curve below T_g(PS) in Figure 2 along the logarithmic time axis, that is, by transforming $t_{\mathrm{eff}} = a_T^{-1}t$. The reference temperature is taken as the lowest temperature investigated, that is, 4.25 °C for 14% PS and 6.3 °C for 17% PS, such that all curves are shifted to the positive log-time direction. This plot illustrates that time−temperature superposition works reasonably well below T_g(PS). In contrast, we were unable to include the data above 70 °C on the same master curve by time−temperature superposition of any kind, clearly manifesting the expected change in physical properties of the material. However, although the data in the elastomeric regime below T_g(PS) do allow a unique time−temperature superposition, we find more evidence of an abrupt change in behavior at around 30 °C by examining the values of time shift factor a_T.

The traditional way to analyze time−temperature superposition is to apply the so-called WLF equation.[19] This famous empirical law has a strong physical background and works well in a great variety of polymeric systems. However, even at the first glance, the WLF approach is ambiguous in a multicomponent system with two widely separated glass transitions, such as our SIS copolymer. The experimentally determined time

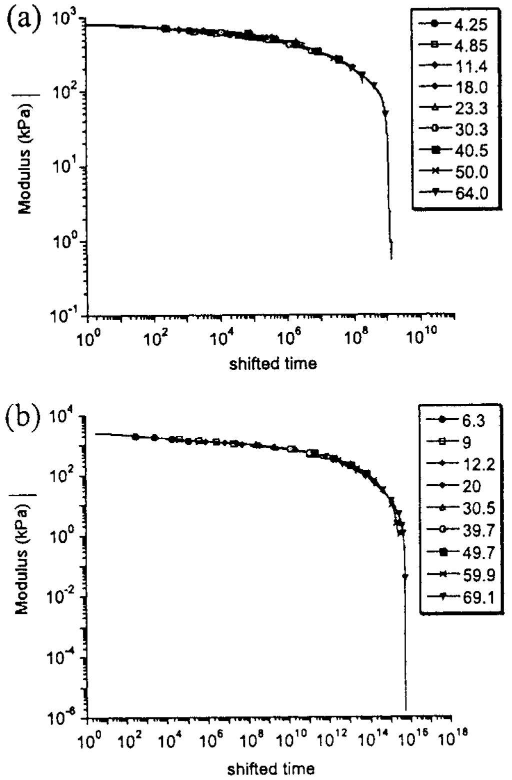

Figure 3. Master curves of the stress relaxation of SIS elastomer below T_g(PS), obtained by time−temperature shift $t_{\text{eff}} = a_T^{-1}t$ from the data in Figure 2 for the 14% PS sample (a) and 17% PS sample (b). The similarity of the two master curves is striking, despite the difference in cross-linking morphology. One can distinguish the power-law relaxation regime at lower temperatures (shorter times) and a faster $E(t)$ variation at long times (higher temperatures, but still below T_g).

shift factors a_T for each of the stress relaxation curves below 70 °C are plotted against the temperature in Figure 2. The shift factors are seen to increase with increasing temperature on a log scale; however, at a crossover temperature around 30 °C (303 K), one finds an evident change in behavior. To illustrate this, we attempted to fit the WLF equation[19]

$$\log a_T = \frac{C_1(T - T_{\text{ref}})}{C_2 + T - T_{\text{ref}}} \qquad (1)$$

where C_1 and C_2 are the empirical coefficients. The values of C_1 and C_2 are often quoted in pure materials as $C_1 = -17.44$ and $C_2 = 51.6$ when the reference temperature is taken as the glass transition point T_g. The original WLF paper[19] takes T_{ref} approximately 50° above the corresponding T_g and obtains $C_1 = -8.86$ with $C_2 = 101.6$. In our case the reference temperature for the 14% PS sample was was $T_{\text{ref}} = 4.25$ °C and for the 17% PS sample 6.3 °C, approximately 50° above T_g(PI), which should be the relevant glass transition for this WLF analysis. We find that only the data below 30 °C would fit this equation, with WLF coefficients of $C_1 = -17.44$, $C_2 = 240$ for 14% PS and $C_1 = -7.24$, $C_2 = 6.55$ for the 17% PS sample (shown as a solid line in Figure 4). Clearly, there is no significance in these rather random figures. To illustrate, the dashed line shows an attempted fits of all a_T points to a WLF equation—obviously an unsuccessful attempt.

3.2. Relaxation Law. We now proceed to analyze the stress relaxation itself. As the assembled plots in Figures 2 and 3 suggest, the $E(t)$ data for the lowest temperatures follows a simple power law. This would be expected of a cross-linked polymer network,[1−3] especially taking into account a high probability of free dangling ends in a phase-separated triblock copolymer system. In the region below 30 °C both samples have their stress relaxing according to

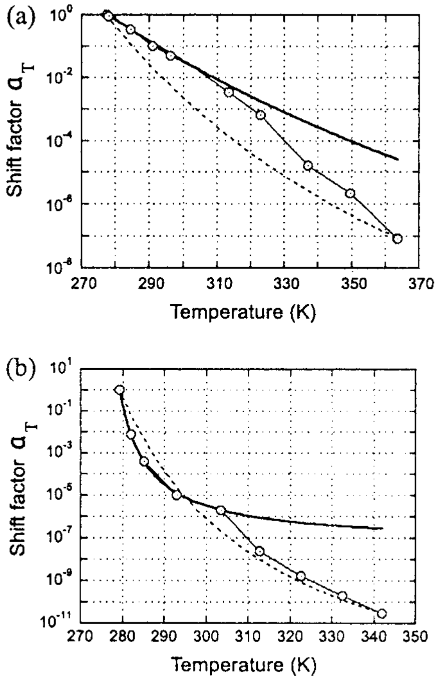

Figure 4. Time shift factors a_T used to collapse the relaxation data on the master curves Figures 3, against the temperature, for the samples 14% PS (a) and 17% PS (b). Solid lines show the attempted WLF fit of the points below $T^* \sim 30$ °C; dashed lines show the attempted WLF fit of all a_T points.

$$E(t) \approx E_0(1 + 1.6t^{-0.12}) \quad \text{for 14\% PS}$$

$$E(t) \approx E_0(1 + 2.2t^{-0.15}) \quad \text{for 17\% PS} \qquad (2)$$

with only E_0 a fitting parameter. Significantly, all curves for a given material can be fitted with the same power-law exponent of 0.12 or 0.15 and prefactor of ≈1.6 or 2.2.

At higher temperatures, above T^*, or, equivalently, at longer times on the master curves, the stress relaxation becomes much faster. From 39 to 70 °C, the stretched exponential law becomes the only reasonable model that can fit the data for both samples:

$$E(t) \approx 835 \exp[-(t/\tau)^{0.2}] \quad \text{for 4\% PS}$$

$$E(t) \approx 1088 \exp[-(t/\tau)^{0.2}] \quad \text{for 17\% PS} \qquad (3)$$

As with the low-temperature regime, all curves for a given sample can be fitted with only one fitting parameter, τ. The stretched exponent index has the same value of 0.2 for all experimental runs, for both samples; only the characteristic time scale τ depends on the temperature. The last relaxation curves, obtained at temperatures above 50 °C, eventually reached zero stress during the experiment, corresponding to zero net elastic response; other plots also go to zero when extrapolated to $t \to \infty$. One could say that in this temperature range the samples respond thermoplastically to an applied strain. The relaxation time, τ, plotted against temper-

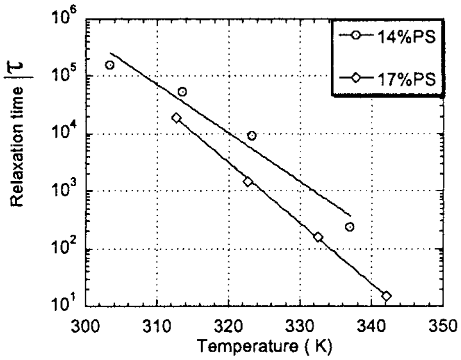

Figure 5. Relaxation time $\tau(T)$, a parameter of stretched exponential law (3) at high temperatures. Solid lines show the fit of each data set by the simple exponential $\tau = \eta \exp(-\alpha T)$, with $\alpha = 0.19$ and 0.24 for 14% PS and 17% PS samples, respectively.

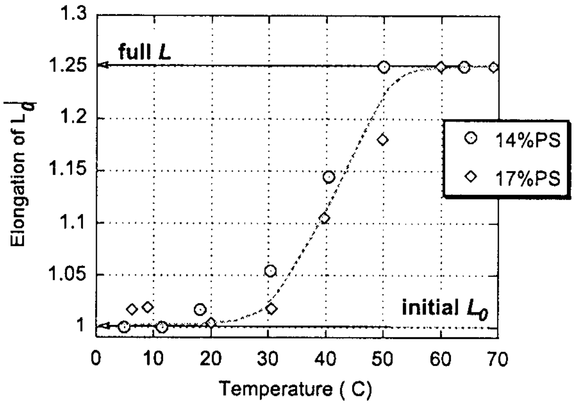

Figure 6. Changes in the natural length L_0 of SIS samples after the 2 day relaxation at different temperatures below T_g(PS). Below T^* all samples returned to their original shape, showing a fully elastic response; above T^* the samples suffered increasing amounts of plastic deformation, eventually creeping irreversibly to the full extended length $L = 1.25L_0$. The broken line is a guide to the eye, illustrating the amount of creep at different temperatures.

ature in Figure 5, drops dramatically with increasing the temperature (in accordance with the time shift constant a_T in WLF analysis), indicating that the relaxation time is going to be faster at higher temperature.

To reiterate the contrast between the two temperature regions, we attempted to fit the higher-temperature relaxation curves with a power law and the lower-temperature curves with a stretched exponential—the result has very clearly been negative, so we were left with no doubt that the suggested time evolution regimes are unique in each of these distinct temperature regions.

3.3. Natural length L_0. The changes in the length of SIS samples before and after the stress relaxation experiments were also recorded and are given in Figure 6. The data for both samples clearly highlight the turning point at 30 °C, before which samples behave almost completely elastically and after which samples experienced more plastic flow as the test temperature increased toward T_g(PS). However, significantly, at all temperatures we find that the effective total cross-linking density remains the same. The decrease of actual or extrapolated stress to zero is achieved by the altering the natural length L_0 and thus reducing the effective strain applied to the sample. If, after the end of relaxation experiment, we determine the new natural length L_0' (as shown in Figure 6) and stretch the sample again by 25% with respect to this new value, the stress magnitude and relaxation are the same as during the first run. This indicates that the total number of effective cross-links in the SIS network remains the same and suggests the probable leading mechanism of relaxation in the regime below T_g(PS) but above $T^* \sim$ 30 °C. Under stress, the PS chains can be pulled out of the micelles, which are still in a fully glassy state. Remarkably, this mechanism appears to be the same and produce very similar results, for both the cubic phase of spherical PS micelles and the hexagonally packed cylindrical aggregates. This chain pullout relieves the local stress and allows the sample to change shape. However, after mechanical equilibration, the free PS chain does not stay in the predominantly PI matrix but finds another PS micelle to link with. The rate of this recombination process seems to be much faster than the release rate, since the free PS chains are diluted in the molten PI matrix and thus have high mobility, until they link with a new glassy PS micelle. Then, when a new strain is applied, the newly shaped material responds with the same elastic modulus $E(t)$: this process is analogous to remolding of SIS samples. The main novel result of this work is that the nature of PS glass appears to change abruptly at around 30 °C, below which no chain pullout takes place on the experimental time scale, and accordingly, the sample sustains the finite stress in equilibrium and preserves its shape elastically. Significantly, this appears to be independent of the particular microstructure of the phase-separated material.

4. Discussion

Above the glass transition of PS micelles, the SIS blend behaves viscoelastically, and $E(t)$ curves appear to follow the rapidly decaying power law $E(t) \approx g_{\mathrm{visc}}(t/t_{\mathrm{v}})^{-1/2}$, as indicated in Figure 2. This means that the stress relaxation curves at different temperature above the T_g(PS) are also going to be superimposed, but with a different set of reference temperature and parameters. This latter fact has also been reported by Chung et al.[20] One can easily understand that the phase separation creates an energy barrier, which holds the soft PS chain segments in the (molten) spherical or cylindrical micelles and thus creates an effective cross-link for the PI network. At higher temperatures this energy barrier becomes weak and insufficient to resist the elastic force. This is one of the obvious transitions on raising the temperature.

The reasons for a distinct break in behavior at a crossover point T^* in the elastomeric regime well below T_g(PS) are less obvious. According to the phase diagram of PS−PI blend, the block copolymer will not be completely phase-separated microscopically. Rather the material will split into two regions one of which is a micelle of PS-rich phase and the other a continuous matrix of PI-rich phase. This partial miscibility is the main origin of the variation in the measured T_g of the copolymers compared to corresponding homopolymers. Simple combining rules for copolymers[20] suggest that the T_g of a combination is of the form

$$\frac{1}{T_g} = \frac{x}{T_g(1)} + \frac{1-x}{T_g(2)}$$

where x is the weight fraction, which could be used to estimate the concentration of free PS in the PI matrix:

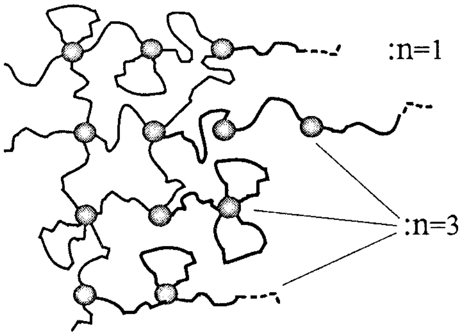

Figure 7. Sketch illustrates the free dangling ends naturally occurring in the SIS elastomer network (on the example of cubic phase of 14% PS copolymer). In the first case there is a single SIS chain attached to only one PS micelle, which itself is a part of the network: $n = 1$. The case of $n = 3$ is presented in different variations: a linear conformation and a number of possible loops, all assumed to contribute similarly to the individual dynamics of the retracting strand.

the change from −63 to −55 °C for PI requires $x \sim 8\%$ of PS impurity. This means a significant amount of freely dangling chain ends in the otherwise effectively cross-linked PI network; see the sketch in Figure 7 (which also shows a possibility of a dangling end terminated with a loop). This is consistent with the power-law stress relaxation of a fully elastic rubbery state that we observe at low temperatures. Characteristically, and also consistently with the physical picture of the thermoplastic SIS elastomer at low temperatures, the power-law exponent of 0.15 is very close to that reported experimentally in the classical studies of rubber relaxation[22] and also theoretically attributed to the relaxation of free dangling ends.[3]

To directly apply the theoretical ideas of stress relaxation due to the retraction of free dangling chains attached to the percolating network, one needs to make a minor modification of the Curro et al. argument. We assume that, if the probability of one triblock copolymer chain to be attached to the network is $\tilde{q}$, the probability of having n such triblock segments to form a free dangling end is $P(n) = \tilde{q}(1 - \tilde{q})^{n-1}$ (see Figure 7). Then, following the concept of[3] that the relaxing part of stress is proportional to the part of the retracting chain that has not yet relaxed to equilibrium, $\Delta\sigma(t) \sim nL - l(t)$, with $\nu = nL$ the total number of monomers in the chain, we write for the relaxation modulus:

$$\begin{aligned} E(t) &= E_0 + \kappa \sum_{\nu=1}^{\infty} [\nu - l(t)]\tilde{q}(1 - \tilde{q})^{\nu/L-1} \\ &= E_0 + \kappa \frac{\tilde{q}(1 - \tilde{q})^{1/L-1}}{(1 - (1 - \tilde{q})^{1/L})^2}(1 - \tilde{q})^{1/L} \qquad (4) \end{aligned}$$

Taking the de Gennes' estimate for the retracting time $l(t) = a \ln(t/\tau)$, one obtains after rearrangement, in full analogy with Curro et al.,

$$E(t) = E_0[1 - (t/\tau_{\mathrm{av}})^{-a\tilde{q}/L}] \qquad (5)$$

with E_0 the equilibrium value of the modulus at $t \to \infty$ and the relaxation time τ_{av} determined by the $\tilde{q}$-dependent prefactor in eq 4.

Above 30 °C, the stress relaxation switches to a completely different mechanism and follows a stretched exponential law. Such time dependence is known in other physical systems characteristic of quenched collective behavior and indicates a broad distribution of relaxation times. Having in mind the idea of PS chains being pulled out of the glassy micelles, one can understand this changed relaxation mechanism by comparison with the free chain end retraction discussed above. At any given time t a new population of free dangling ends is added to the system (proportional to the probability of PS chain pullout at a given temperature and applied force[23]). Simultaneously, the effective natural length L_0 is increased by the same proportion, thus reducing the effective strain and the force applied to the remaining network strands. Such a collective mechanism of self-retardation leads, in our case, to a slow stretched-exponential stress decay to zero (or a very low stress value, below the pullout threshold of PS micelles). What is most unusual is that such transformation occurs some 40 deg below the glass transition within PS micelles acting as effective network cross-links, T_g(PS) unambiguously identified by thermal and mechanical means.

Two models mentioned above describe different regimes of network behavior, with permanent and with breakable cross-links. However, analyzing our experimental data, it is interesting to note that *all* stress relaxation curves below T_g(PS) are superimposed on the master curve in Figure 3, despite the apparent change in physical properties around T^*. This change does not imply that there is some kind of structural or phase change in SIS polymer networks at this temperature, well below the glass transition of PS micelles. According to DSC, there is no evidence of any thermal signature at T^* in equilibrium. In fact, since the mechanical relaxation data below and above the crossover T^* are falling onto the same master curve, we could assume that they represent the *same* universal relaxation law but at very different characteristic time scale, depending on the temperature of relaxation experiment. If we assign a characteristic time τ_{PS} of a PS chain pullout from a glassy matrix, such a time must be a function of applied force, the length of PS chain trapped in the micelle, and the temperature.[23] Then, at a given temperature, the stress relaxation experiment may remain in the time window much smaller than τ_{PS}: the network would appear permanently cross-linked, as our results below T^*, modeled by the power-law relaxation (5). At a higher temperature τ_{PS} could decrease such that a significant proportion of PS chains rearrange during the period of experiment: we obtain a corresponding stretched exponential relaxation above T^*.

To summarize, this work has provided detailed stress relaxation measurements on SIS block copolymers over a range of temperatures. It provides a different look at the symmetric triblock copolymer systems acting as thermoplastic elastomers from that of Sato et al.[13] and particularly focuses on the low-PS-containing materials with no solvent. As expected, the behavior changes from that of a classical polyisoprene rubbery network, held together by glassy polystyrene micelles, to that of a viscoelastic polymer melt, when the molten PS blocks are not capable of sustaining the stress. However, we also find a marked change in behavior much below T_g(PS), at around 30 °C, when the strength of glassy PS regions becomes less and the chain pullout and reassembly take place under sufficient force. The fact that our findings for cubic and hexagonal phase separation morphology in the copolymer melt are qualitatively similar to those of Sato et al. (in 50% solvent, with likely

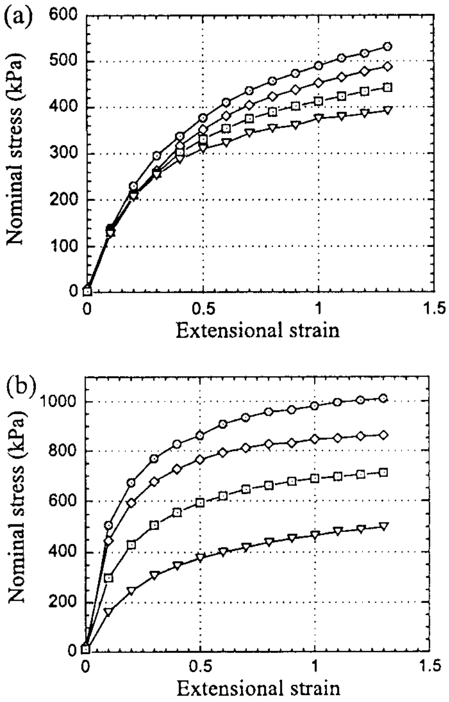

Figure 8. Stress−strain relations for the 14% PS sample (a) and the 17% PS sample (b) obtained at a fixed temperature near the crossover $T^* \sim 30$ °C and increasingly slow strain rates: 0.4, 0.1, 0.0166, and 0.0025 min^{-1} for circles, diamonds, squares, and triangles, respectively.

different morphology) suggests that the mechanical relaxation mechanisms discussed here are indeed universal and should be relevant to a broad range of other thermoplastic elastomers.

Acknowledgment. This research is supported by the Bridgestone Corporation (A.H.) and EPSRC UK (S.M.C.). We appreciate discussions with J.-F. Joanny, P. G. de Gennes, A. R. Tajbakhsh, and especially A. J. Ryan, whose help in obtaining and interpreting the structural data from synchrotron SAXS was invaluable.

Appendix: Stress−Strain Relations and Relaxation

The equilibrium stress−strain behavior is an important characteristic of rubber properties. Even though our work is concerned with relaxation mechanisms at a relatively small fixed strain, it is necessary to examine the response at different deformations to identify the regime of study. Accordingly, we have performed a series of stress−strain measurements at different rates of strain increase.

It is immediately obvious that the question of equilibrium stress−strain response is rather ambiguous. Even before the experiment, it is expected from the concept of PS chain pullout that we put forward in this article that all SIS materials at all temperatures would eventually creep to the state of zero stress. Therefore, the rate at which strain is imposed is crucial for the outcome stress. The data sets in Figure 8 indicate this for both materials studied. Four strain rates are shown: 6.7×10^{-3} s^{-1} (circles), 1.7×10^{-3} s^{-1} (diamonds), 2.8×10^{-4} s^{-1} (squares), and 4.2×10^{-5} s^{-1} (triangles). The effect of strain on internal mechanical relaxation is qualitatively the same in both samples, with fcc and hexagonal morphology, but is more pronounced in the more rigid 17% PS material.

Essentially, there is no linear equilibrium stress−strain regime in SIS rubber. It may appear that in the temperature range below $T^* = 30$ °C the linear response is observed, but this is only the question of time allowed for relaxation, as the master curves indicate. Similarly, although curves in Figure 8 appear linear at strains below 10%, this is only a result of too fast strain rate. The slowest rate of $\sim 10^{-5}$ s^{-1} shows deviations even in this region. On increasing magnitude of strain the relaxation rate is clearly accelerating. At very high strain all materials creep very significantly, even at the lowest temperatures studied. These observations are, in fact, consistent with the concept of chain pullout from the glassy PS micelles. If one assumes the pullout rate τ_{PS} to follow an energy barrier activation law, then the increasing strain would shift and decrease the barrier: $\tau_{\text{PS}} \propto \exp[(W - {}^1\!/_2\kappa\epsilon^2)/kT]$. Accordingly, the crossover temperature T^* should move to lower values at higher deformations imposed. Testing this in greater detail was outside the scope of this paper.

References and Notes

(1) Chasset, R.; Thirion, P. In *Proceedings of the Conference on Physics of Non-Crystalline Solids*; Prins, J. A., Ed.; North-Holland Publishing Co.: Amsterdam, 1965; p 345.
(2) Ferry, J. D. *Viscoelastic Properties of Polymers*; John Wiley & Sons: New York, 1980.
(3) Curro, J. G.; Pincus, P. *Macromolecules* **1983**, *16*, 559.
(4) Curro, J. G.; Pearson, D. S.; Helfand, E. *Macromolecules* **1985**, *18*, 1157.
(5) Dickinson, E. *Introduction to Food Colloids*; Clarendon: Oxford, 1992.
(6) Ross-Murphy, S. B. *Ber. Bunsen-Ges. Phys. Chem.* **1998**, *102*, 1534.
(7) Clement, F.; Johner, A.; Joanny, J.-F.; Semenov, A. N. *Macromolecules* **2000**, *33*, 6148.
(8) Thomas, D. K. *Polymer* **1966**, *7*, 125. Clark, A. H.; Ross-Murphy, A. H. *Adv. Polym. Sci.* **1987**, *83*, 57.
(9) Flory, P. J. *Trans. Faraday Soc.* **1960**, *56*, 722. Tanaka, F.; Edwards, S. F. *Macromolecules* **1992**, *25*, 1516.
(10) Bates, F. S. *Annu. Rev. Phys. Chem.* **1990**, *41*, 525.
(11) Hasegawa, H.; Tanaka, H.; Yamasaki, K.; Hashimoto, T. *Macromolecules* **1987**, *20*, 1651.
(12) Papers in: *Developments in Block Copolymers*; Goodman, I., Ed.; Applied Science Publishers Ltd.: Oxford, 1982.
(13) Sato, T.; Watanabe, H.; Osaki, K. *Macromolecules* **1996**, *29*, 6231.
(14) Watanabe, H.; Sato, T.; Osaki, K.; Yao, M. L.; Yamagishi, A. *Macromolecules* **1997**, *30*, 5877.
(15) Clarke, S. M.; Terentjev, E. M. *Faraday Discuss.* **1999**, *112*, 325.
(16) Keddie, J. L.; Jones, R. A. L.; Cory, R. A. *Faraday Discuss.* **1994**, *98*, 219.
(17) de Gennes, P. G. *Eur. Phys. J. E* **2000**, *2*, 201.
(18) Kawasaki, K.; Onuki, A. *Phys. Rev. A* **1990**, *42*, 3664.
(19) Williams, M. L.; Landel, R. F.; Ferry, J. D. *J. Am. Chem. Soc.* **1955**, *77*, 3701.
(20) Chung, C. I.; Gale, J. C. *J. Polym. Sci., Polym. Phys. Ed.* **1976**, *14*, 1149.
(21) Elias, H.-G. *Macromolecules*; Plenum Press: New York, 1977; Vol. 1, p 411.
(22) Dickie, R. A.; Ferry, J. D. *J. Phys. Chem.* **1966**, *70*, 2594.
(23) Krupenkin, T. C.; Taylor, P. L. *Macromolecules* **1995**, *28*, 5819.

MA001976Z